the aid of Eqs. (5) and (9) gives

$$\frac{q - q_f}{q_E - q_f} = 1 - \frac{[(\Gamma_w)^2 + 4(1 + \Gamma_w + 21\,\Gamma_g)]^{1/2} - \Gamma_w}{2(1 + \Gamma_w + 21\Gamma_g)} \tag{11}$$

where, for the stagnation region of axisymmetric bodies,

$$\Gamma_w = \frac{(\rho_w K_w)Sc^{2/3}}{(0.47)\,[2(\rho_e\mu_e)_0\beta C]^{1/2}} \tag{12}$$

Equation (11) is a closed form solution that gives the heat transfer ratio $(q - q_f)/(q_E - q_f)$ for arbitrary-rate simultaneous gas-phase and surface reactions.

The terms Γ_g and Γ_w, defined by Eqs. (8) and (12), are essentially Damkhöler numbers representing the ratio of characteristic diffusion time to characteristic chemical reaction time for the gas-phase and surface reactions, respectively.

Discussion

The accuracy of the solution, Eq. (11), cannot be checked for the arbitrary combinations of Γ_g and Γ_w because the general exact solutions are not available. It can be established that the equation gives correct results at the two limiting cases of either $\Gamma_g = 0$ or $\Gamma_w = 0$. It is sufficiently accurate when $\Gamma_w = 0$, because Γ_g was obtained by matching the results with the solutions of Ref. 9. It is correct also when $\Gamma_g = 0$, because the solution (11) essentially becomes the solution of Ref. 3. Though there is no direct check in the intermediate region, it is felt that the physical reasoning leading to the equivalent surface reaction concept of Eq. (10) is sound. The excellent correlation shown for the gas-phase reaction with noncatalytic surface appears to support the accuracy of the results presented.

The variation of $(q - q_f)/(q_E - q_f)$ with respect to Γ_g and Γ_w, as given by Eq. (11), is seen in Fig. 1. The general behavior is similar to that for the Couette flow obtained in Ref. 10.

It is noted here that the same problem considered here also is being studied by Inger[11] from a different approach. In his analysis the production term, or the source term, in the formal diffusion equation is approximated by a simpler function requiring only a correct matching near the surface. It is therefore based on a concept similar to that used herein in that the chemical state near the surface is assumed to be of controlling influence. It is still, however, an approximate analysis, and the accuracies of any of these approximate analyses can be checked only when exact solutions become available.

Conclusions

The concept of equivalent surface reaction has been developed for gas-phase recombination at the stagnation region of blunt bodies. This concept is based on the fact that the chemical state of a nonequilibrium highly cooled boundary layer is determined largely by the recombination that occurs near the wall. An equation based on this concept was shown to predict the heat transfer to a noncatalytic surface to within a few percent of the more accurate existing results. The equation was generalized to apply to the case in which surface catalytic recombination occurs simultaneously with gas-phase reaction. The present solution, which is in a simple closed form, should be useful in estimating heat transfer, although the accuracy of the solution cannot be checked for the general case, because of a lack of exact solutions. The atom concentration profile across the boundary layer can be obtained from the value m_w obtained herein, since in a frozen boundary layer the profile is determined when m_w is known (for instance, see Ref. 3), and the present theory is, in essence, based on the frozen boundary layer theory with modification only in the boundary condition at the surface. The profile thus obtained should approximate the true profile with the same degree of accuracy as the heat transfer results. This profile, in turn, defines the chemical state across the boundary layer. The equivalent surface reaction concept will be extended to flow fields beyond the stagnation point of a blunt body.

References

[1] Fay, J. A. and Riddell, F. R., "Theory of stagnation point heat transfer in dissociated air," J. Aerospace Sci. **25**, 73–85, 121 (1958).

[2] Chung, P. M. and Anderson, A. D., "Heat transfer around blunt bodies with nonequilibrium boundary layers," *Proceedings of the 1960 Heat Transfer and Fluid Mechanics Institute* (Stanford University Press, Stanford, Calif., 1960), pp. 150–161.

[3] Goulard, R. J., "On catalytic recombination rates in hypersonic stagnation heat transfer," Jet Propulsion **28**, 737–745 (1958).

[4] Chung, P. M. and Anderson, A. D., "Heat transfer to surfaces of finite catalytic activity in frozen dissociated hypersonic flow," NASA TN D-350 (1961).

[5] Chung, P. M., "Shielding stagnation surfaces of finite catalytic activity by air injection in hypersonic flight," NASA TN D-27 (1959).

[6] Scala, S. M., "Hypersonic stagnation point heat transfer to surfaces having finite catalytic efficiency," *Proceedings of the U. S. National Congress of Applied Mechanics* (Am. Soc. Mech. Engrs., New York, 1958), pp. 799–806.

[7] Inger, G. R., "Correlation of surface temperature effect on nonequilibrium heat transfer," ARS J. **32**, 1743–1744 (1962).

[8] Rae, W. J., "An approximate solution for the nonequilibrium boundary layer near the leading edge of a flat plate," Inst. Aerospace Sci. Paper 62-178 (June 1962).

[9] Goodwin, G. and Chung, P. M., "Effects of nonequilibrium flows on aerodynamic heating during entry into the earth's atmosphere from parabolic orbits," *Advances in Aeronautical Sciences* (Pergamon Press, New York, 1961), Vol. 4, pp. 997–1018.

[10] Chung, P. M., "A simplified study on the nonequilibrium Couette and boundary-layer flows with air injection," NASA TN D-306 (1960).

[11] Inger, G. R., "Nonequilibrium-dissociated stagnation point boundary layers with arbitrary surface catalycity," Aerospace Corp. Rept. ATN-63(9206)-3 (1963).

Subsonic Wing Span Efficiency

Richard C. Frost* and Robbie Rutherford†
General Dynamics/Fort Worth, Fort Worth, Tex.

THE rather arbitrary manner in which subsonic wing span efficiency often is selected has led to the development of an empirical method by which a more realistic and consistent value of efficiency can be determined. This method depends on a parameter R that is defined as the ratio of the actual chord force to the theoretical chord force with full leading-edge suction; R is found to be a function of leading-edge-radius Reynolds number. This note describes 1) the correlation of R with Reynolds number, and 2) the method for applying the results.

Figure 1 shows the results of plotting R vs Reynolds number with the characteristic length taken as the leading-edge radius at the wing mean aerodynamic chord. All of the data are for wings with symmetrical airfoils; R is determined as follows:

1) The drag at lift is given by

$$C_L^2/\pi\mathcal{A}e = C_c\cos\alpha + C_N\sin\alpha \tag{1}$$

With the usual assumption of small α and with $C_N = C_L/\cos\alpha$ Eq. (1) becomes

$$C_L^2/\pi\mathcal{A}e = C_c + C_L^2/C_{L\alpha} \tag{2}$$

Received January 2, 1963.

* Aerodynamics Group Engineer, Aeroscience Group.

† Aerodynamics Engineer, Aeroscience Group.

Table 1 Wind tunnel data used in R correlation

SYMBOL	NACA REF.	AR	Λ_{LES} (DEGREES)	NACA AIRFOIL	REYNOLDS NO. X 10^{-6}	MACH NO.
○	RML51K26	3.78	49	65A006	2.9,4.4,5.2,6.1	0.10
△	RMA53A30	2.0	45	0003-63	8.0,1.9,4.8	0.61,.24
				0005-63		
				0008-63		
□	RMA51D02	3.0	48.5	64A010	2.0,4.0,8.0,12.0,18.0	0.24
▽	RMA51G31	3.0	48.5	64A010	4.0,6.0,8.0,12.0,18.0	0.25,.60
◇	RML53F24	2.31	60	65A002	5.7	0.17
				65A006		
⊕	RML52A29	2.0	47	65A006	3.32,4.52	0.40,.60
⊕		4.0			2.04,2.77	0.40,.60
⊕		6.0			1.58,2.13	0.40,.60
▽	RMA53C20	2.0	56.31	0005-63	3.0	0.24,.61
○	RMA50K27	10.0	35	65_1A012	2.0,4.0,6.0,10.0	0.25
●		5.0	35	65_1A012	2.0,4.0,6.0,10.0	0.25
▶	RML52K21	4.0	45	65A006	1.62	0.40,.60
▼	TN 4397	2.0	60	65A008	1.02	0.13
▼		4.0			0.72	
▼		6.0			0.59	
×	RML51H13	8.0	46.33	63_1A012	1.62,2.2,3.0,4.8	0.07→0.25
⊕	RMA50A04a	2.0	63.43	0005(MOD)	15.3	0.13
⊗	RML56G02	3.7	45	[a] t/c = .086	0.93	0.06
◇	RML50F16	4.0	45	65A006	1.5,3.0,4.5	0.20
⊠	RML51J04	8.0	45	63_1A012	1.5,2.2,3.0,4.0	0.19
⊕	RML56A10	3.7	47.8	[a] t/c = .083→.090	1.8	0.13
◇	RMA8D20	3.5	63	64A006	3.55	0.16,.30,.60
■	RML53E20	4.0	45	65A006	1.90 - 3.0	0.40,.50,.60
◁	RMA54J20	3.0	53.1	0003-63	3.0	0.62
◡	TN 3529	4.0	27	63A008	1.7 (1.4→2.0)	0.60
			18	63A006		
			15	63A004		
⊕	RMA53J14a	3.0	53.1	0003-63	3.8	0.60
✳	RMA55D11	3.0	45	64A006	2.90	0.60
⊕	RMA50K20	2.0	63.43	0008-63	3.0,5.0	0.60
☆	RMA51D27	5.0	43	64A010	2,3,4,6,10	0.25,.40
□	RMA8D02	3.5	63	64A006	8.0	0.125

[a] Not standard NACA sections.

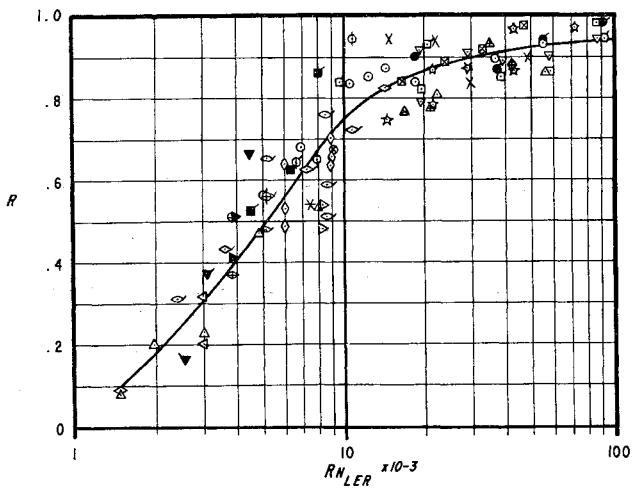

Fig. 1 Correlation of R with Reynolds number; R values for $M \leq 0.6$

or the chord force from Eq. (2) is given by

$$C_c = C_L^2[(1/\pi \mathcal{A}e) - (1/C_{L\alpha})] \quad (3)$$

2) Theoretically, with full leading-edge suction and elliptic span loading, the wing span efficiency e becomes 1.0, and Eq. (3) reads

$$C_c = C_L^2[(1/\pi \mathcal{A}R) - (1/C_{L\alpha})] \quad (4)$$

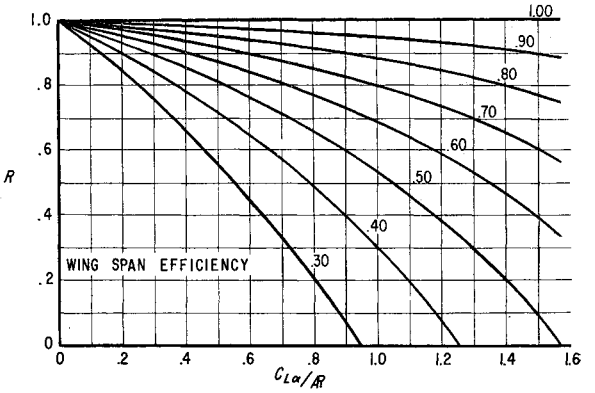

Fig. 2 Wing span efficiency calculation plot

3) The ratio of Eq. (3) to Eq. (4) gives R:

$$R = \frac{\pi - (C_{L\alpha}/\mathcal{A}Re)}{\pi - (C_{L\alpha}/\mathcal{A}R)} \quad (5)$$

This quantity was computed using wind tunnel results obtained on a large number of wings with a broad range of sweep angles, aspect ratios, taper ratios, thickness ratios, and Reynolds numbers as indicated in Table 1. The correlation of Fig. 1 was terminated at 0.6 Mach, where effects due to compressibility began to appear in the data.

The results show a very well-defined trend of increasing R with increasing leading-edge-radius Reynolds number. No

consistent variations due to the geometric parameters are evident in the scatter about the faired curve. Hence, it is concluded that the curve is a good statistical average with the scatter being similar to results obtained when investigating other viscous phenomena.

The curve of Fig. 1 can be used directly to predict the span efficiency of wings, or it can be used as a guide to extrapolate results from wind tunnel tests to full scale. It is especially useful in this regard when model data are available on an actual design where some of the leading-edge suction may be eliminated. For example, fuselages, nacelles, or other components may blanket the wing leading edge locally, thus preventing the possibility of developing suction in such regions.

Above a leading-edge-radius Reynolds number of 100,000, it has become customary to use $R = 0.95$. Upon checking, it was found that this value yields span efficiencies that closely agree with an empirical method used by Sheridan[1] for full-scale aircraft.

The span efficiency e may be computed from Eq. (5) as follows:

$$e = \frac{(C_{L\alpha}/\mathcal{A}\mathrm{R})}{R(C_{L\alpha}/\mathcal{A}\mathrm{R}) + (1 - R)\pi} \tag{6}$$

This expression is plotted in Fig. 2. The significance of the results now becomes apparent. For example, for a fixed value of R, e increases as the ratio of $C_{L\alpha}/\mathcal{A}\mathrm{R}$ increases. Thus, the wing that produces more $C_{L\alpha}$ per unit aspect ratio will have a higher span efficiency. This fact becomes important in design work and makes the selection of a wing planform and airfoil section take on well-defined significance, since the wing planform geometry is implicit in the value of $C_{L\alpha}$.

The approach of this note with suitable modifications could be extended to higher Mach numbers, including supersonic Mach numbers for wings with subsonic leading edges.

[1] Sheridan, H. G., "Aircraft preliminary design methods used in the Weapons System Analysis Division," Navy Dept., Bur. Naval Weapons Rept. R-5-62-13 (June 1962).

Approximate Method for Calculating the Compressible Laminar Boundary Layer with Continuously Distributed Suction

W. Pechau*
Institute of Fluid Mechanics of the Technical University, Braunschweig, Germany

CONTROL of the compressible laminar boundary layer by continuously distributed suction may be employed on airfoils either at small angles of incidence to avoid transition to turbulence and thus to reduce skin friction or at larger angles of incidence to prevent separation and thus to increase the maximum lift. The presumed existence of a laminar boundary layer on the impermeable wall is based on the reduction of density with altitude, so that even at high speeds requiring the consideration of compressibility the critical Reynolds number is not exceeded.

Received by IAS November 9, 1962.
* Research Collaborator.

A rational calculation of compressible boundary layers can be achieved only by an approximation of the Pohlhausen type. Whereas for impermeable walls some integral methods are available,[1] no method of general validity for the case of suction or blowing has been established as yet. In a recent paper[2] a method was presented which has, for the present, been restricted to the special case of an adiabatic wall and a Prandtl number of unity, because for this case a universal relationship between the velocity and temperature profiles exists. In this note a brief account of the method is given.

The method is based on the momentum-integral equation with a pertaining compatibility condition at the wall.[3] The assumption for the velocity profile is of a form

$$u(x,y)/U_e(x) = f[\eta(x,y), K(x)] \tag{1}$$

Here $K(x)$ is a shape factor of the profiles and

$$\eta = \int_0^y \frac{\rho}{\rho_e}\, d\left[\frac{y}{\delta_1(x)}\right] \tag{2}$$

with $\delta_1(x)$ denoting a scale factor proportional to the local boundary layer thickness. The velocity profile used here is composed of an exponential term that reproduces the asymptotic suction profile correctly and a sine term that well approximates the flat-plate profile without suction. The same analytic expression had been used by Schlichting[4] for the incompressible case.

After the introduction of Eq. (1) into the momentum-integral equation, the momentum-loss thickness

$$\vartheta = \int_0^\infty \frac{\rho u}{\rho_e U_e}\left(1 - \frac{u}{U_e}\right) dy \tag{3}$$

in the substituted form

$$Z^* = (\vartheta/l)^2(R/l)^2(U_\infty l/\nu_\infty)$$

is calculated from the equation

$$dZ^*/dx^* = F_1(x^*)\cdot G(k,k_1) + F_2(x^*)\cdot k$$

with

$$k = F_3(x^*)\cdot Z^* \qquad k_1 = F_4(x^*)(Z^*)^{1/2} \tag{6}$$

The quantities F_1 to F_4 are explicit functions of the coordinate $x^* = x/l$ along the chord, which implies a dependence on the external velocity $U_e(x)$, the local Mach number $M_e(x)$, the radius of curvature $R(x)$, and, for F_4, on the suction velocity $v_w(x)$. The shape factor $K(x)$ occurring in Eq. (1) is obtained from a relation

$$K = K(k,k_1) \tag{7}$$

Having thus determined the velocity profile for each position x, the other characteristic parameters such as displacement thickness and skin friction are evaluated easily. The temperature profile is connected with the velocity profile through the general relation just mentioned. For incompressible flow, the method reduces to the one given by Schlichting.[4]

The practical computation is complicated by the fact that the quantity $G(k,k_1)$ occurring in Eq. (5) is not an explicit function of k and k_1. Therefore, Truckenbrodt[5] introduced a linearized form of this function into the incompressible method of Schlichting. Employing such a linearization here also, one obtains, instead of Eq. (5),

$$dY^*/dx^* = A(x^*) - B(x^*)(Y^*)^{1/2} \tag{8}$$

with

$$Y^* = \left(\frac{\vartheta}{l}\right)^2\left(\frac{U_e}{U_\infty}\right)^6\left(\frac{R}{l}\right)^2\left(\frac{T_e}{T_\infty}\right)^{[2(2-\varkappa)/(\varkappa-1)]}\frac{U_\infty l}{\nu_\infty} \tag{9}$$

The quantities A and B are explicit functions of $U_e(x)$, $M_e(x)$,